Plasmonic Nanocavity Organic Light-Emitting Diode with Significantly Enhanced Light Extraction, Contrast, Viewing Angle, Brightness, and Low-Glare

*Wei Ding, Yuxuan Wang, Hao Chen, and Stephen Y. Chou**

One central challenge in LEDs is to increase light extraction; but for display applications, other factors may have equal significance, such as ambient-light absorption, contrast, viewing angle, image sharpness, brightness, and low-glare. However, current LED structures enhance only some of the factors, while degrading the others. Here, a new organic LED (OLED) structure is proposed and demonstrated, with a novel plasmonic nanocavity, termed "plasmonic cavity with subwavelength hole-array" (PlaCSH), and exhibits experimentally significant enhancements of all above factors with unprecedented performances. Compared to the conventional OLEDs (the same but without PlaCSH), PlaCSH-OLEDs achieve experimentally: i) 1.57-fold higher external-quantum-efficiency and light-extraction-efficiency (29%/32% without lens, 55%/60% with lens)—among the highest reported; ii) ambient-light absorption not only 2.5-fold higher but also broad-band (400 nm) and nearly angle and polarization independent, leading to lower-glare; iii) fivefold higher contrast (12 000 for 140 lux ambient-light); iv) viewing angle tunable by the cavity length; v) 1.86-fold higher normal-view-brightness; and vi) uniform color over all emission angles. The PlaCSH is an excellent optical antenna—excellent in both radiation and absorption of light. Furthermore, PlaCSH-OLEDs, a simple structure to produce, are fabricated using nanoimprint over large-area (≈1000 cm^2), hence scalable to wallpaper size.

1. Introduction

For display image quality, in addition to light extraction,[1–20] the LED's ambient light absorption (reflection), contrast, viewing angle, image sharpness, brightness, and low-glare are all important.[21–35] In the displays for hand-held devices (the largest usage of displays), which are viewed at a fixed angle and are often used in bright ambient light, these factors may be more important than light extraction. However, the current LED structures improve only some of the factors, often at the expenses of degrading the others. For examples, the most common methods for enhancing light extraction (i.e., light scattering/reflection using micro/nano-patterned surfaces/interfaces and/or metal mirrors)[3–5,7–9,11–20,36–39] often significantly increase the ambient light reflection, hence degrading the contrast. Such ambient light reflection problem is particularly serious in OLEDs (which use metallic high-reflective backplanes)[22–24] or high light extraction inorganic LEDs (flip-chip with metallic high reflective-mirror).[10] All current methods for good contrast uses the methods that absorb the ambient light (e.g., circular polarizers, light absorbing layers, destructive-interference buffer layers, and low light reflection black cathode)[22–24,26–34] but also degrade the light extraction substantially. The light extraction degradation is often as large as a factor of 2 (i.e., lossing a half of the total light that is otherwise being extracted). In other words, the most current LED structures cannot have high light extraction and high ambient light absorption (i.e., low ambient light reflection) at the same time; they are either a good light radiator or a good ambient light absorber, but not both. Resonant-cavity LEDs with dielectric mirrors can be a good light radiator and absorber, but only in a few nanometer wavelength range and in a particular direction,[37,40] hence suffering similar low contrast and large glare as other LED structures in display applications. Moreover, in conventional LEDs, the viewing angle is fixed by the Lambertian radiation pattern unless using lenses or resonant cavities;[41] and the ambient light reflection often follows Fresnel's law, hence having large glare.

Metals have many unique properties over dielectric counterparts. One of them is the generation of surface plasmon polariton (SPP), which can, under certain conditions, enhance the light radiation rate (Purcell Effect), alter the radiation intensity and pattern, and improve the light extraction.[42,43,55,56] Yet, the implementation into LEDs with a single layer of metallic (plasmonic) structures (either nanostructures or a planar thin-film)[44] or two layers of planar metallic thin-films has achieved only limited improvements in LED light extraction.[36] The general concept of using a plasmonic microcavity with nanoperforated metal cladding for improving light extraction was first proposed and discussed theoretically by Barnes,[43] and was implemented experimentally, with limited enhancements, to the optical pumped inorganic LEDs with a metal nanograting

W. Ding, Y. Wang, H. Chen, Prof. S. Y. Chou
Department of Electrical Engineering
Princeton University
Princeton, NJ 08544, USA
E-mail: chou@princeton.edu

DOI: 10.1002/adfm.201400964

cladding[45] and the electrical pumped OLEDs with a metal hole-array cladding of a period larger than the wavelength[46] (Note: In optically pumped LEDs, the enhancements in light extraction and absorption are intertwined and cannot be separated experimentally, and hence cannot be quantified individually).[45] However, there are no studies or proposals on the use of plasmonic effects to improve LED's ambient light reflection, contrast, viewing angle, brightness and glare.

Recently, we proposed and developed a new ultra-thin solar cell using a novel subwavelength plasmonic nanocavity, termed "plasmonic cavity with subwavelength hole-array" (PlaCSH), which shows high (>90%) light absorption and trapping over a broad bandwidth and omni acceptance (nearly independent of incident light angle and polarization and with changes much smaller than Fresnel law).[47] Our previous experiments also show that the blocking of the light transmission through the subwavelength holes in a thin metal mesh by covering each hole with an opaque metal disk nearby, in fact, does not block the light at all, but instead significantly enhance light transmission than the open holes.[48] Based on these experiments and an expectation of reciprocity in plasmonics, we have implemented the broad-band subwavelength plasmonic nanocavity, PlaCSH, into light emitting devices.

Here, we present the design, fabrication, simulation, and performance of a new electrical-pumped OLED, PlaCSH-OLED. The new OLEDs use the plasmonic cavity having deep subwavelength nanostructures that have not been studied before; as a consequence it is able to significantly enhance all the above factors important to display at the same time with unprecedented performances. Namely, the new OLEDs enhance both the light extraction and constrast without sacrifying image sharpness, drastcially different from the conventional LEDs which enhance the light extraction while sacrifying the contrast and image sharpness, or enhance the contrast while scarifying luminance. The work also provides the first direct experimental proof that a plasmonic nanocavity is excellent in both light radiation and absorption, at the same time, for the same wavelength, over a broad bandwidth, and nearly for all incident angles and polarizations (namely, omni radiation/acceptance enhancement).

2. PlaCSH-OLED Structure, Principle, and Design

The PlaCSH-OLED has a novel subwavelength plasmonic nanocavity, PlaCSH, that comprises a top light-transmissive metallic-mesh electrode with subwavelength hole-array (MESH) as one of two cladding layers of the plasmonic cavity, a planar opaque metallic back electrode as another cladding layer, and in between light emitting materials. The cavity length, defined as the light emitting material thickness, is less than a half of the emission wavelength. The MESH also plays the role of replacing the conventional (indium-tin-oxide) ITO front transparent electrode. In PlaCSH-OLED operation, holes and electrons are supplied by the MESH electrode and the Al back electrode, respectively; and are recombined in the light emitting materials to generate photons (light). In this work, the PlaCSH-OLEDs were fabricated face-down with MESH next to the substrate through which the light comes out.

In an optimized PlaCSH-OLEDs fabricated, the MESH is 15-nm-thick Au mesh with a 200 nm period hole array of 180 nm hole diameter and an AuOx atomic layer on its surface; the back electrode is 0.3 nm thick LiF and 100 nm thick Al films; and the light emitting materials comprise 80 nm thick green phosphorescent host–guest materials of 4,4',4''-tris(carbazol-9-yl) triphenylamine (TCTA) as the hole transporting material, and 4,7-diphenyl-1,10-phenanthroline (BPhen) as the electron transporting material; both are uniformly doped with a phosphorescent guest, fac-tris(2-phenylpyridine) iridium(III) [$Ir(ppy)_3$] (**Figure 1**). The PlaCSH-LED's total thickness without a substrate is 195 nm.

With the phosphorescent guest $Ir(ppy)_3$, both the singlet and triplet states are used for light emitting,[1] thus the internal quantum efficiency is high and estimated to be ~ 92% for our devices (see later). The light emitting materials have a luminescence peak at 520 nm and an index of 1.65–1.70. The substrate used is a 1.46 index fused-silica. The 200 nm period of the MESH, which is less than the peak wavelength in the light emission material (λ/n = 306 nm), matches well with the surface plasmon wavelength in the plasmonic cavity (an over-simplified model: $\lambda = \lambda_0/\sqrt{\varepsilon_m \varepsilon_a / (\varepsilon_m + \varepsilon_a)}$, which gives ≈200 nm for λ_0 = 520 nm light at the Au and active layer interface, which has a permittivity of ε_m and ε_a). To reduce non-radiative loss (e.g., Joule loss) in MESH, both the thickness and width are kept in deep subwavelength size (15 nm and 20 nm respectively), but still maintaining a good lateral DC electrical conductivity. Many of the rules and specific parameters in designing the PlaCSH-OLED are based on our previous experiments in PlaCSH-solar cells and related plasmonic nanostructures.[47,48]

The key functions of the plasmonic nanocavity, PlaCSH, are to, as shown later, a) drastically enhance the effective light extraction to outside over broadband and hence EQE; b) significantly increase the absorption of the ambient light over a broad bandwidth and all incident angles and polarizations, hence leading to a significant enhancement of the contrast and low-glare; and c) control the far-field radiation patterns, hence enhancing the viewing angles and brightness.

3. Fabrication

The PlaCSH-OLEDs were fabricated on 4" fused silica substrates (0.5 mm thick) using planar or roll nanoimprint lithography (NIL)[49,50] (Figure 1c). The 4" NIL molds with the mesh patterns of 200 nm period and different hole sizes over the entire mold were fabricated using a combination of interference lithography and then multiple NIL, etching, self-perfection, and mold duplication[49,51] (Note, in some cases, a large-area flexible roll-to-roll mold (50 cm × 20 cm) was used to fabricate large area MESHs).

Specifically, the MESHs on the substrates were first fabricated on a substrate by NIL and the deposition and lift-off of 15 nm thick Au, followed by an UV-ozone treatment to form an atomic thick AuOx on top. Then the layers of 40 nm thick TCTA and 40 nm thick BPhen, both 2 wt% $Ir(ppy)_3$ doped, (all materials are commercial products from Sigma Aldrich, used as received) were sequentially evaporated thermally onto the MESH under ~10^{-7} Torr without breaking vacuum. Finally, the

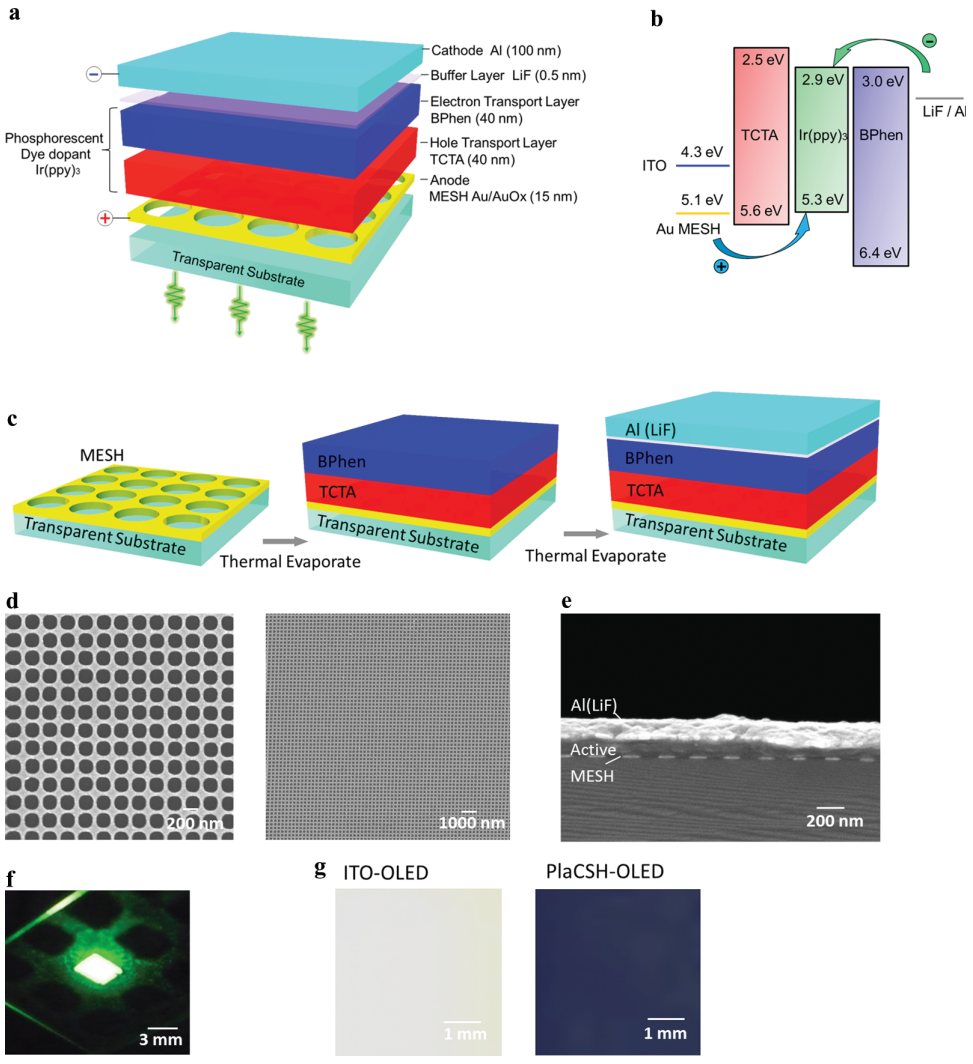

Figure 1. Organic light emitting diode (OLED) of plasmonic cavity with subwavelength hole-array (PlaCSH). a) Structure schematic: a top (Au) metallic-mesh electrode with subwavelength hole-array (MESH), a back electrode (LiF/Al), and in between thin layers of green phosphorescent organic host–guest materials: BPhen and TCTA (both $Ir(ppy)_3$ doped); b) energy band diagram; c) fabrication process: fabrication of MESH by nanoimprint on a transparent substrate, deposition of organic active materials, and thermal deposition of LiF and Al electrode; (d) scanning electron micrograph (SEM) of 15 nm thick Au MESH with a hole array of 200 nm pitch and 180 nm diameter; e) cross-sectional SEM of PlaCSH-OLED (the non-uniformity of Al layer was created during cleaving the sample for SEM); photographs of (f) green light emission from PlaCSH-OLED and g) ambient light reflection of reference ITO-OLED (white) and PlaCSH-OLED (dark blue).

LiF (0.5 nm) and Al (100 nm) films were evaporated through a shadow-mask, which defines the back electrode and hence the OLED active area (3 mm by 3 mm).

Scanning electron microscopy (SEM) shows that the MESH indeed has a 200 nm pitch, 180 nm hole diameter, a hole shape close to square with round corners and smooth edges, and excellent nanopattern uniformity over large area (Figure 1d). It also shows that due to a thin thickness of MESH, the organic films on top have rather smooth surface and cover the MESHs well without any observable pin-holes (Figure 1e).

For comparison, also fabricated were the references, "ITO-OLEDs", which are the same LEDs as the PlaCSH-OLEDs except that the MESH is replaced by an ITO layer (100 nm thick). The electrical testing shows that the MESH has a sheet resistance 8 Ohm/sq –20% lower than the ITO layer (10 Ohm/sq).

4. Electroluminescence and Broadband, Omni Enhancement

The spectra of the front-surface total electroluminescence of both PlaCSH and ITO-OLEDs were measured as a function of bias (injection current) using an integrated sphere (Labsphere LMS-100) and a spectrometer (Horiba Jobin Yvon), and were calibrated using a lump standard (Labsphere AUX-100). During the measurements, the backside and the four edges of all the LEDs were fully covered with black-tapes to ensure the light emission only from the LEDs' front surface.

The measured spectra show that the front-surface total electroluminescence (EL) intensity of PlaCSH-OLEDs is much higher than ITO-OLEDs over the entire measured wavelength range (480 nm to 640 nm). For example, at 10 mA/cm^2

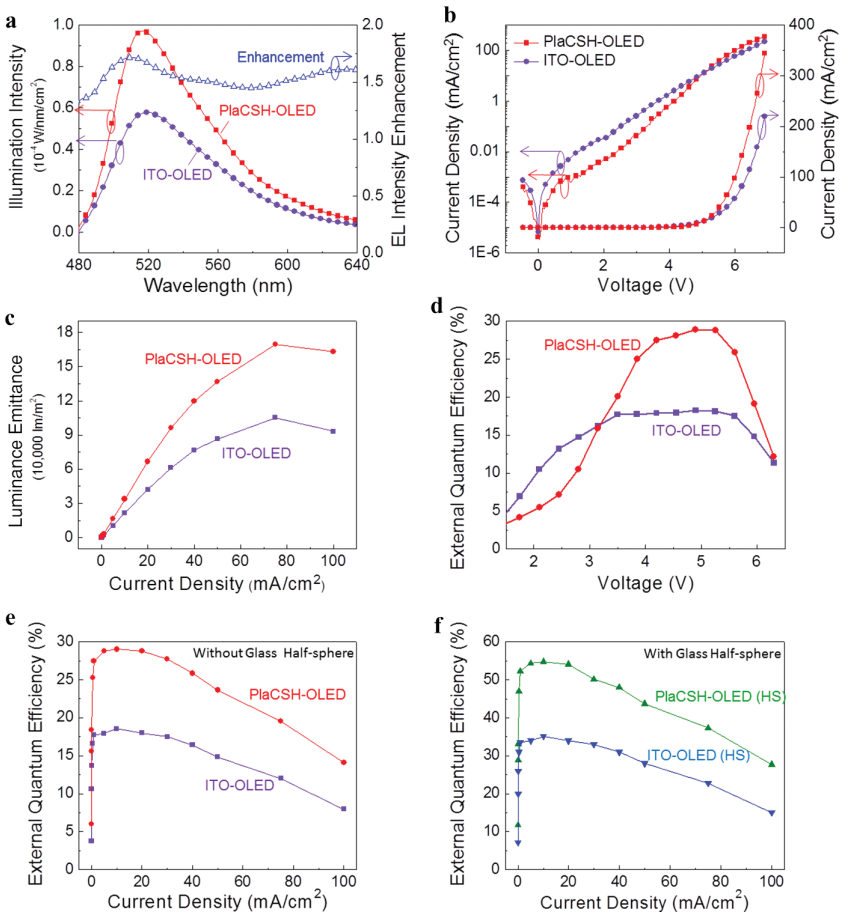

Figure 2. Measured electro-luminance (EL), *J–V*, Luminous Emittance and EQE of PlaCSH-LEDs and ITO-LEDs. a) Total front-surface EL/enhancement spectrum at 10 mA/cm^2 current density, b) current density vs voltage (*J–V*), c) luminous emittance vs current density, d) EQE vs voltage, and EQE vs current density e) without and f) with glass half-sphere. Compared to ITO-LEDs, PlaCSH-LEDs has an EL peak of 1.69-fold higher and 3 nm blue shift, and an EQE (at 10mA/cm^2) of 29.1% and 54.5% for without and with the glass half-sphere, both are 1.57-fold higher than ITO-OLEDs (18.5% and 35%).

current density, the PlaCSH-OLED's EL has the maximum of 1×10^{-4} W/(nm cm)^2 at 517 nm wavelength and a total of 6.7×10^{-3} W/cm^2 integrated over the entire measured spectrum, which is 1.69- and 1.57-fold higher than ITO-OLEDs (0.6×10^{-4} W/(nm cm)^2 and 4.3×10^{-3} W/cm^2), respectively (**Figure 2**).

The measurements also clearly show that the EL enhancement by PlaCSH (i.e., the ratio of the spectrum of PlaCSH to ITO OLEDs) is broadband: nearly constant (within ±8%) over the entire 160 nm measured wavelength range. However, the actual PlaCSH's enhancement bandwidth should be much wider, since the EL measurement is limited by the bandwidth of the emission material. A linear superposition analysis would easily prove that the near constant enhancement over a broad wavelength band means that the radiation enhancement is nearly independent of the wavelength, radiation angle, and polarization of the original radiation inside the PlaCSH, namely "omni radiation enhancement".

The PlaCSH-OLED's EL spectrum has the peak at 517 nm to 3 nm blue shifted from ITO-OLED (520 nm peak), and a bandwidth of 61–7 nm (10%) narrower than ITO-OLED (68 nm). The slight blue shift and slight narrower bandwidth are attributed to the slight variation in the EL enhancement spectra of PlaCSH at the light emitting wavelength range.

5. Current Density–Voltage Characteristics and Luminous Emittance Enhancement

The current density vs voltage (*J–V*) characteristics were also measured (Figure 2b). Compared to ITO-OLEDs, the PlaCSH-OLEDs, although having a similar turn-on voltage of 2.4 V @10cd/m^2 (versus 2.3 V for ITO-OLEDs), have i) much larger current increasing slope (i.e., larger differential conductance) and hence a larger current above the threshold (e.g., 70% larger at 6 V); and ii) a smaller leakage current in both forward and reverse bias (e.g., 10-fold smaller at +2 V and 1.8-fold smaller for –0.5 V), which are also smaller than the OLED for the same material system reported previously.[54]

The high current in PlaCSH-OLEDs is attributed to hole-injection-barrier height lowering by the AuOx electrode layer over an ITO layer. The less leakage current in the PlaCSH-OLEDs than the ITO-OLEDs is attributed to less pinholes in the organic material layers that cover the MESH (as indicated in our SEM inspection).[52]

Using the measured EL spectra-vs-bias and J-V, we obtained the light luminous emittance vs the injection current (*L–J*) or the bias (*L–V*), by integrating the EL spectra for a given current or bias with the eye's luminosity function as the weight and dividing the device area (Figure 2c,d). The *L–J* shows that PlaCSH-OLEDs have much higher luminous emittance than ITO-OLED, reaching 34 000 lux (=lm/m^2) at 10 mA/cm^2 and a maximum of 170 000 lux at 75 mA/cm^2, which is 1.56- and 1.62-fold higher than that for ITO-OLEDs (22 000 lux and 105 000 lux).

6. External Quantum Efficiency and Power Efficiency Enhancement

The front-surface external quantum efficiency (EQEs) as a function of bias voltage or injection current were obtained from the measured EL spectra-vs-bias and *J–V* (Figure 2e,f). At the injection current range from 1 mA/cm^2 to 100 mA/cm^2, the PlaCSH-OLED has an EQE of a maximum of 29.1% (at 10 mA/cm^2 (4.8 V))—1.57-fold higher, and an average of 25%—1.6-fold higher than ITO-OLED (a max EQE of 18.5% and an average of 15.6%). The enhancement in EQE by PlaCSH is the same as

Table 1. Radiation Properties of PlaCSH-OLED and ITO-OLED

	EQE[a)]	EQE[a)] (with HS)	Maximum Power Efficiency	Normal Direction Brightness[a)]	Viewing Angle	Central Wavelength	Bandwidth	Light Extraction Efficiency (LEE)	
	[%]	[%]	[lm/W]	[cd/m^2]	[°]	[nm]	[nm]	without HS [%]	with HS [%]
ITO-OLED	18.5	35.0	107	7300	118	520	68	20	38
PlaCSH-OLED	29.1	54.5	150	13000	100	517	61	32	60
Enhancement [%]	**57**	**56**	**40**	**78**	—	—	—	**57**	**56**

[a)]Under current density of 10 mA/cm^2.

that in EL, indicating again that the enhancement by PlaCSH is broadband and nearly independent of wavelength and polarization over the EL spectrum. The EQE is, to our best knowledge, the highest for the OLEDs on 1.46 index glass substrate without a lens and for any substrates when the index is scaled.

To release the light trapped in the planar fused-silica substrate, an uncoated half-sphere (HS) (B270 glass of 1.51 index which is slightly higher than the substrate) was placed on the substrate surface opposite to the LEDs with a thin matching liquid layer (an index identical to the substrate) in between. The HS has a 10 cm diameter, much larger than the LED's size (3 mm), and the LEDs were placed at the HS's focal point. With the HS, the measured maximum EQE is increased to 54.5% from 29.1% for PlaCSH-OLED, and 35% from 18.5% for ITO-OLED. The increase is 1.87- and 1.89-fold for each type of LEDs, respectively, which is essentially the same (Figure 2g and **Table 1**). The measured EQE can be further increased by having a higher internal quantum efficiency and better index matching between the HS and the substrate (e.g., the current EQE for PlaCSH-OLEDs can become 84% for 100% IQE and a perfect index matching).

The maximum wall-plug power efficiency is 80/150 lm/W for PlaCSH-OLEDs without/with a lens, which is ≈1.43-fold higher than ITO-OLEDs (56/106 lm/W). The power efficiency can be significantly increased by, in addition to increasing EQE, lowering turn-on voltage.

7. Internal Quantum Efficiency and Light Extraction Efficiency Enhancement

For the ITO-OLEDs, light extraction efficiency (η_{extr}), obtained from the well-tested ray-optics model, is 20%;[53] thus giving the internal quantum efficiency (IQE) for our LEDs of 92%, since the measured EQE is 18.5% and IQE = EQE/η_{extr}.

For PlaCSH-OLEDs, the Purcell effect in light radiation enhancement should be small, because the IQE without PlaCSH is already 92%. We lump the Purcell effect into the η_{extr} in the equation of IQE = EQE/η_{extr}. Based on the measured EQEs and the estimated IQE, the effective light extraction efficiency of PlaCSH-OLEDs is 32% and 60%, respectively without and with HS. They are 1.57-fold higher than ITO-OLED (20% and 38%), and are the highest of light extraction reported for index 1.46 glass substrate and any substrate when the index is scaled.[4,5] If an index perfectly matched and lossless lens is used, the estimated light extraction efficiency for the ITO-OLED and PlaCSH-OLED on 1.46 index substrate will be increased to 54% and 84% (Table 1).

8. Angular Dependence of EL, Spectra, and Luminance (Brightness)

The angular dependences of EL spectra of all LED types were measured using a rotation stage, a collimation lens and a photodetector. The lens with 5 mm diameter was 5 cm away from the LEDs, thus having a 0.008 sr acceptance angle. By integrating the EL spectra over the wavelength with the luminosity function as the weight and dividing it by the acceptance solid angle and the device area, the luminance versus emission angle was obtained (**Figure 3**, **4**), which shows several things particularly interesting.

First, in the ITO-LEDs, the luminance angle distribution is nearly independent of the cavity length and has a viewing angle fixed at ~120°, as expected, since the conventional LED's emission angle distribution is always close to the Lambertian.[41] But for PlaCSH-OLED, the angle distribution and hence the viewing angle, strongly depend on the cavity length: it can be either narrower or wider than the Lambertian (Figure 3). Specifically, using 80 and 120 nm cavity length, the PlaCSH-OLED's viewing angle is 100° and 138°, respectively, ≈17% narrower and wider than the ITO-OLED's of the same cavity length, giving a total viewing angle tunability of 38°; while the ITO-OLED viewing angle is 118° and 122°, only having 4° tunability. The viewing angle tunability per cavity length change in the current PlaCSH-LED is 1°/nm. The narrower (wider) viewing angle means higher (less) percentage of light in the normal forward direction.

Second, the measured EL spectra of PlaCSH-OLED show being independent of the emission angle, namely, uniform color over angle (COA), highly desired in displays, just as ITO-OLED (Figure 4). Again, the uniform COA provides another experimental evidence of the omni radiation enhancement nature of PlaCSH. In previous light extraction enhancement approaches of replacing the ITO electrode with thin metal film(s) (e.g., dielectric-metal-dielectric (DMD) layers) or using dielectric resonant cavities, the LEDs have a poor COA.[37] This indicates again that the PlaCSH is a fundamentally different type of cavity and is based on a different physical principle from previous approaches.

Third, while ITO-OLEDs having a Lambertian light emission distribution and hence an angle independent luminance (i.e., brightness), the luminance of the PlaCSH-OLED can become angle dependent. For the 80 nm cavity length PlaCSH-OLED (having 100° viewing angle), the luminance at the normal angle (which is the most relevant angle to the displays for hand-held devices) is 13 000 cd/m^2 at 10 mA/cm^2 and 65 000 cd/m^2 at

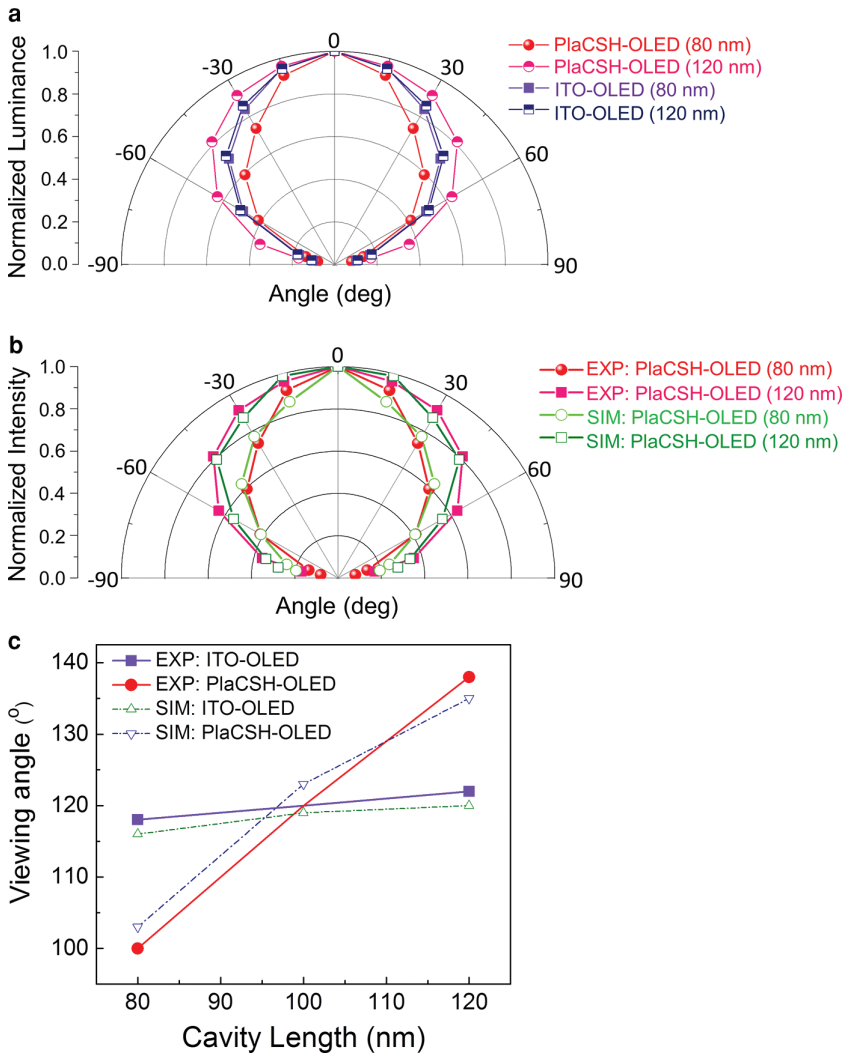

Figure 3. Angular distribution of electro-luminance (EL) of PlaCSH-OLED and ITO-OLEDs with various cavity lengths (80 nm and 120 nm). a) Normalized luminance vs angle, b) comparison of measurements with FDTD simulations, and c) measured and simulated viewing angle vs cavity length. Experiments show that when the cavity length is changed from 80 to 120 nm, the viewing angle is virtually fixed (120°) for ITO-OLED, but for PlaCSH-OLEDs it is changed drastically from 100° to 138° with ≈1°/nm tunability (viewing angle/cavity length change). The simulations fit experiments within 5%.

75 mA/cm^2, which is 1.78- and 1.86-fold brighter than the ITO-OLED (7300 cd/m^2 and 35 000 cd/m^2) (Figure 4a,b). These enhancements come from 1.57-fold higher light extraction (hence EQE) and 1.17-fold viewing angle narrowing (more light in the forwarding direction).

9. Broad Band, High, Omni Absorption (Low Reflection) to Ambient Light

The absorptions (reflections) of ambient light by the LEDs were measured with a white light source as well as the light standard, collimation optic, and spectrometer similar to the previously described. A striking feature of PlaCSH-OLEDs is that the absorption (hence reflection) to ambient light is not only much higher (lower) than ITO-OLEDs; but more importantly, it is broadband, and nearly angle and polarization independent up to 30° and afterward a dependence far less than that predicted by Fresnel's law (which is termed "Omni acceptance"), making it have far less glare and higher contrast.

Specifically, the ambient light reflectance spectra of OLEDs measured at normal incident and 300 to 900 nm wavelength range show 1) the PlaCSH-OLEDs have a minimum reflectance of 8.3% at 720 nm wavelength, an average of 26%, and luminous reflectance of 25% (average over the luminosity function and CIE standard illuminant D65, see below), which is, respectively, 5.6-, 2.8-, and 2.7-fold smaller than that of the ITO-OLEDs (a minimum reflectance of 45% at 450 nm, an average of 70%, and a luminous reflectance of 67%) (**Figure 5**a); and 2) the bandwidth for the low ambient light reflection (high absorption) is 400 nm for PlaCSH-OLEDs ≈4.4-fold wider than 90 nm for ITO-OLEDs. The ambient light absorption/reflection properties are also clearly seen in the photographs of the PlaCSH and ITO-OLEDs taken at normal direction under white light (Figure 1).

The luminous reflectance in the paper was calculated by:

$$R_{\mathrm{L}} = \frac{\int_{\lambda_1}^{\lambda_2} V(\lambda) S(\lambda) R(\lambda) \mathrm{d}\lambda}{\int_{\lambda_1}^{\lambda_2} V(\lambda) S(\lambda) \mathrm{d}\lambda}$$

where $V(\lambda)$ is the standard photonic curve (eye's luminosity function), $S(\lambda)$ is the CIE standard illuminant D65, $R(\lambda)$ is the reflective spectrum, λ_1 and λ_2 are chosen as 450 and 750 nm.

The ambient light luminous reflectances of OLEDs measured at different angle and polarization show that the luminous reflectances of the PlaCSH-OLEDs are not only much smaller than the ITO-OLEDs, but more importantly, they do not follow Fresnel's law as ITO-OLEDs. Specifically, for the PlaCSH-OLEDs, the s-polarization reflectance is nearly constant at 27% for 0° to 60° angle and then is increased to 37% at 75°; and the p-polarization reflectance is nearly constant at 27% for 0° to 30° angle, then drops with angle, reaching a minimum of 5% at 60° and 10% at 75° (Figure 5b). The s and p-polarization reflectance of PlaCSH-OLED at 60° angle is 3.1- and 5.8-fold less than ITO-OLED (27%:83%, 5%:29%), respectively; and is 2.5 and 3.1-fold less (37%:91%, 12%:37%) at 75° angle. The broadband, Omni high ambient light absorption (low reflection) of PlaCSH-OLEDs also can be seen in the 2D plots of the reflection as a function of both angle and polarization (Figure 5c–f). The ambient light absorption properties of PlaCSH-OLEDs are similar to the PlaCSH-solar cells that we reported previously.[47]

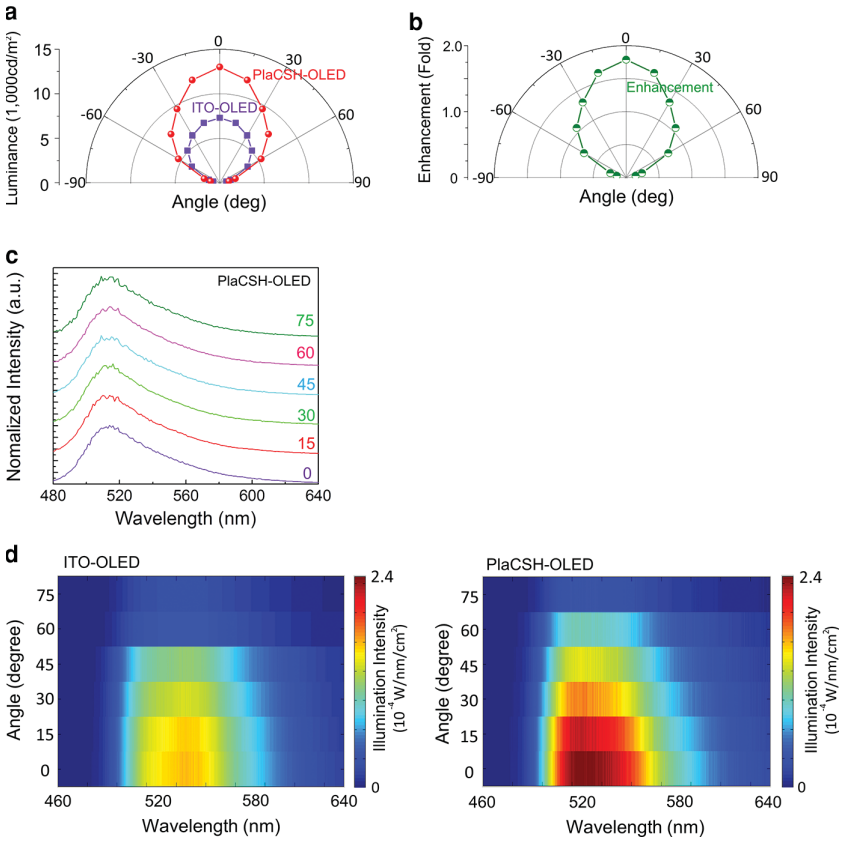

Figure 4. Measured angular distribution of electro-luminance (EL) of PlaCSH-OLED and ITO-OLED with 80 nm cavity length at 10 mA/cm^2 current density. a) Luminance vs angle; b) Luminance enhancement of PlaCSH-OLED over ITO-OLED vs angle; c) normalized EL spectra of PlaCSH-OLED at different angles; and d) EL spectra vs angle and wavelength. Experiments show that PlaCSH-OLED (with 29.1% EQE) has i) luminance at normal direction 78% higher than ITO-OLED, ii) EL spectra independent of angle (i.e., uniform color over angle), and iii) 100° viewing angle ≈17% narrower than ITO-OLED's of the same cavity length (120°). The viewing angle narrowing channels more light to the eyes of a handheld device viewer.

10. Omni Radiation and Absorption Enhancement, EQE-Absorptance Product

In the experiments described above, the enhancement of light radiation and absorption by PlaCSH were measured separately and independently, hence they provide the first direct experimental proof that the plasmonic nanocavity, PlaCSH-OLED, is excellent in both light radiation and absorption over broad wavelength band and nearly independent of incident angle and polarization (omni radiation/acceptance enhancement) (e.g., both excellent optical antenna and optical absorber). The product of LED's EQE and ambient-light-absorptance (EQE-A), a key figure of merit to a display, is 0.21 (29% × 74%) and 0.41 (55% × 74%) for the PlaCSH-OLEDs without or with a lens, which is at least threefold higher than all previous LEDs.[7,33]

11. High Contrast of PlaCSH-OLED

The high light extraction and low ambient light reflection of PlaCSH-OLED lead to a significant enhancement of the contrast, which is defined as:

$$\text{Contrast} = (L_{on} + L_{ambient} \times R_L)/(L_{off} + L_{ambient} \times R_L)$$

where L_{on} and L_{off} is the luminance of the "on" and "off" state, respectively; $L_{ambient}$ is the ambient luminance; and R_L is the luminous reflectance.

From the experiments, we found that, for an ambient luminance range of 0 to 10,000 lux, and a current density range of 1 to 100 mA/cm^2, the contrast (average all polarizations) of PlaCSH-OLED is higher than the ITO-OLED by 4–5-fold for normal incident ambient light, and 3–5-fold for non-normal angle angles (**Figure 6** and **Table 2**).

For example, at the current 10 mA/cm^2, the PlaCSH-OLED has a contrast at 0° angle of 2,300, 330 and 34 respectively for an ambient luminance of 140 lux (typical, family living room), 1000 lux (high, over cast day), and 10 000 lux (full daylight), respectively, all of them are 4–5 times higher than the ITO-OLED (490, 69 and 8). At the current 75 mA/cm^2, the contrasts of PlaCSH-OLED are further enhanced to 12 000, 1600, and 160 for these three typical ambient luminances (Table 2). For different current (1, 10, and 100 mA/cm^2), the contrast of PlaCSH-OLED at 0° angle and 140 lux ambient luminance is 222, 2300, and 11 324, which is also ≈fivefold higher than ITO-OLED (48, 490, and 2102) (Figure 6b). For a different angle of 0°, 30°, 60°, and 75° and at 10 mA/cm^2 current and 140 lux ambient light, the contrast of PlaCSH-OLED reaches 2300, 1523, 1483 and 300, respectively which is 4.7-, 3.5-, 5.1-, and 3.3-fold higher than ITO-OLED (490, 436, 291, and 90). The fivefold higher contrast in PlaCSH-OLEDs comes from the threefold in the lower reflection and the 1.6-fold in the higher EQE/light extraction. The PlaCSH-OLED's ambient light absorption and contrast are also, based our simulations, many times better than OLED structures with the dielectric/metal/dielectric front electrode (Ta_2O_5 (70 nm)/Au (18 nm)/MoO_3 (1 nm)) and an Al back electrode.

12. Simulations and Origin of Enhancements

Using a commercial finite-difference time-domain solver and the geometries, structures and indices of the LEDs from the experiments (except the light emitting material's index has only the real part and hence no absorption), we simulated the PlaCSH-OLED's radiation properties by putting electrical dipole oscillators inside the LEDs, and the absorption properties by sending a plane wave toward the LEDs. The simulated cavity length effects on the OLED's light radiation angle distributions (therefore the viewing angles) are consistent with the experiments within 5% (Figure 3b,c), hence indicating the simulation meaningful.

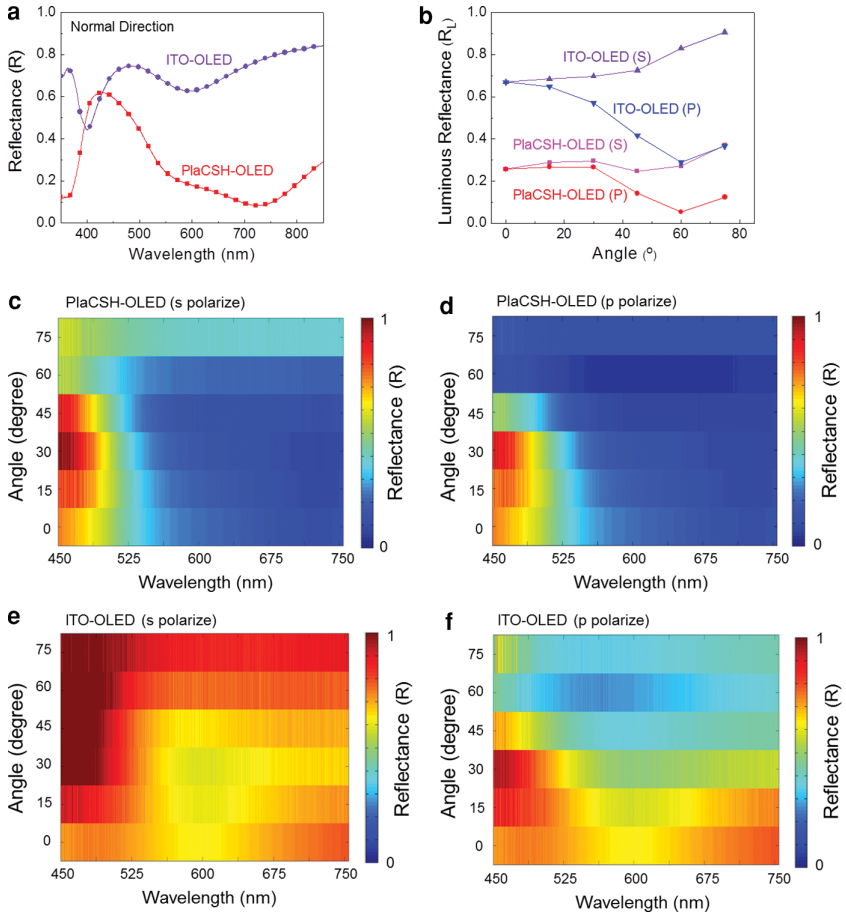

Figure 5. Measured angle and polarization dependence of ambient light reflectance for PlaCSH-OLEDs and ITO-OLEDs. a) Reflectance spectra at normal incidence; (b) luminous reflectance over 450–750 nm wavelength range vs incident angle; and c) reflectance vs wavelength and angle for s and p-polarization, respectively. Experiments show that i) the normal luminous reflectance of PlaCSH-OLEDs is 25%, 3 times smaller than ITO-OLED (67%), and ii) the glare (reflectance from angles) of PlaCSH-OLED is not only over threefold smaller than ITO-OLED, but more importantly nearly independent of light polarization and incident angle, (termed "Omni glare"). For example, at 60°, the luminous reflectance of PlaCSH-OLED is about 3.1- and 5.8-fold smaller than ITO-LED for s and p-polarization (27%: 83%, 5%: 29%), respectively.

Figure 7 shows the simulated radiation of one single dipole (λ_0 = 520 nm) positioned in the middle plane of the light emitting material layer and at a point that is under the middle of either an open-hole or a metal wire of the MESH. The simulations clearly show that the origin of the unique properties of PlaCSH-LEDs (enhancements in LED's light extraction, low-glare, contrast, viewing angle, and brightness) is the localized surface plasmon-polaritons (SPP) generated in PlaCSH.

The simulations show that the PlaCSH is an excellent optical antenna, which radiates the light inside the cavity to outside efficiently (**Figure 7**). Particularly, the simulations show a) unlike the electric field in ITO-OLED which decays monotonically with the distance (as expected for a dipole radiation), the electric field in PlaCSH-OLED is strongly modulated by the periodic metallic nanostructures of MESH, which have much higher electric field near the metal parts than the hole regions of MESH, indicating the dipole radiation being coupled into the SPP of the cavity (the SPP wavelength being determined by the MESH period); b) the SPP in the MESH is localized around the dipole, since not all metal structures but 10–12 periods have a high electrical field; c) the far-field average electric field is relative insensitive to the dipole's locations, indicating again the dipole radiation being coupled into the SPP; and d) the 80 nm cavity length has much stronger radiation to outside than the 300 nm cavity length, indicating strong coupling with a subwavelength cavity length is essential to good light extraction.

For the absorption properties, the simulations further show the PlaCSH is an excellent light absorber: absorbing the light from outside into the PlaCSH cavity efficiently—another key feature of an excellent optical antenna. Particularly, the simulations show a) the ITO-OLED reflects backward the most of the incident light (plane wave) and has only a small portion entered inside the cavity, but the PlaCSH-OLED has most of the incident light entered and trapped inside the cavity and has a very small reflection, even though the PlaCSH has the identical reflective metal backplane; and b) the electric field is uniform in lateral direction (x-direction) in ITO-OLED, but modulated (with the same periodicity as MESH) in PlaCSH-OLED, indicating also the generation of SPP in PlaCSH. The simulations confirm that PlaCSH can be a good light radiator and absorber at the same time.

The PlaCSH-OLED's radiation and absorption behaviors were also simulated in other wavelengths (from 480 to 640 nm range), and were found to be nearly independent of the wavelength, hence broadband.

13. Further Discussions

From the experiments and simulations reported here, it becomes clear that the unique advantages of PlaCSH-OLEDs are due to the unique properties of the PlaCSH structure over other existing LED structures. As pointed out before, previous LED structures (non-resonant cavity structure) cannot be a good light radiator and absorber at the same time; and dielectric resonant-cavity LEDs can be a good light radiator and absorber only in a few nanometer wavelength range and in a particular direction; hence, incapable of enhancing all the critical factors for display applications. On the other hand, PlaCSH is an excellent optical antenna: excellent light radiator and absorber over broad wavelength band and for nearly all light incident angles and polarizations, leading to the enhancements of all critical factors of displays. Such unique properties are due to surface plasmonic polariton generation, the lateral plasmonic momentum fixed by the periodic structure, and the

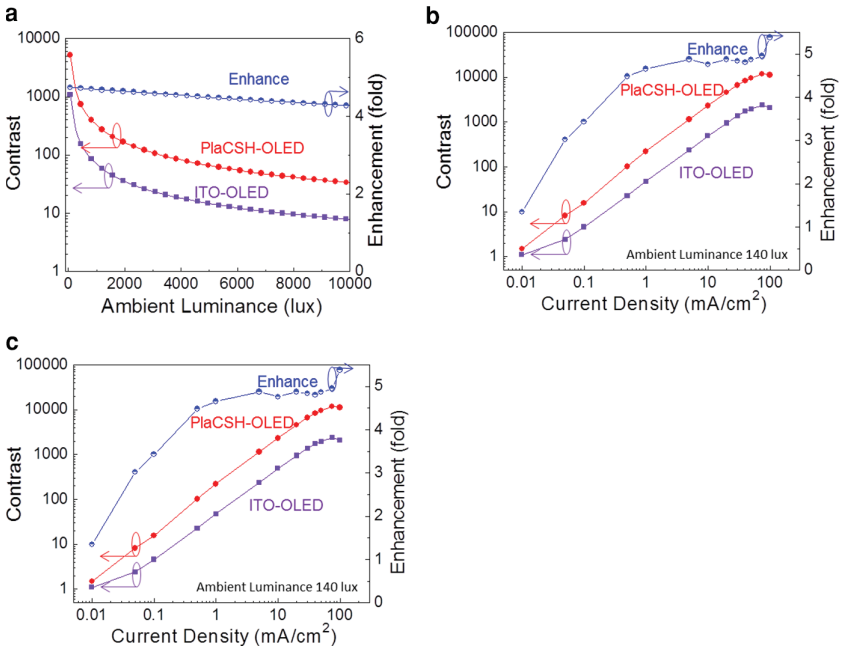

Figure 6. Measured contrast of PlaCSH-OLEDs, and ITO-OLEDs. Contrast versus: a) ambient luminance at zero viewing angle, b) current density, and c) viewing angle of PlaCSH-OLED and ITO-OLED. Other than specified, all ambient luminance are at 140 lux and all OLEDs have 10 mA/cm^2 current density. Experiments show that PlaCSH-OLED's contrast is about 4–5 times higher than ITO-OLED.

wavelength dependence of the metal permittivity (to be detailed elsewhere).

Moreover, another important advantage of PlaCSH is that it has a very simple structure to fabrication, which will greatly reduce the manufacturing cost and increase the yield. In addition, because of replacing the ITO electrode with MESH and having a total thickness less than 200 nm, PlaCSH-OLEDs are very flexible and ductile, and can be potentially made into a fiber form.[7] PlaCSH-OLEDs have already being fabricated by low-cost nanopatterning, nanoimprint to large area (up to 1000 cm^2), hence scalable to wallpaper size. With improvements in materials, structures, or substrate index, the above PlaCSH-OLED's performances can be further improved. The designs, fabrications, and findings are applicable to the LEDs in other materials (organic or inorganic) and on other thin substrates (plastics or glasses), thus opening up new avenues to future high efficiency, high contrast OLEDs and displays.

14. Conclusion

In the work, we proposed and experimentally demonstrated a new organic LED structure that has a novel plasmonic nanocavity, termed "plasmonic cavity with subwavelength hole-array" (PlaCSH), which exhibits the unique properties of being excellent in both light radiation and absorption over broadband (e.g., excellent broad-band optical antenna and optical absorber at the same time), leading to significant enhancement of all the important factors for above LED displays with unprecedented performances. Compared to the conventional OLEDs (the same but without PlaCSH), PlaCSH-OLEDs achieved experimentally: i) 1.57-fold higher front-surface external quantum efficiency and light extraction efficiency (29% and 32% without lens, 55% and 60% with lens)—among the highest reported; ii) ambient light absorption not only 2.5-fold higher (92% max, 74% average), but also broad-band (400 nm) and nearly angle and polarization independent up to 30° and then much smaller changes than Fresnel's law, leading to lower glare; iii) a contrast of five-fold higher (12 000, 1600, and 160 for 140, 1000 and 10 000 lux ambient light) and the highest EQE-absorption-product over previous LEDs; iv) a viewing angle tunable by the cavity length—either narrower or wider than Lambertian (38° tunability demonstrated); v) 1.86-fold higher normal-view brightness (65 000 cd/m^2 luminance at 75 mA/cm^2); vi) 8 Ohm/sq sheet-resistance –20% lower; and vii) uniform color over all emission angles. Therefore, PlaCSH LED is an excellent optical antenna—excellent in both radiation and absorption of light, leading to significantly enhancement of the light extraction, constrast, brightness, and low-glare without sacrifying image sharpness, and drastically different from the conventional LEDs which enhance the light extraction while sacrifying the contrast and image sharpness, or enhance the contrast while scarifying luminance. Furthermore, PlaCSH-OLEDs, a simple structure to fabricate, were fabricated using nanoimprint over large area (up to 1000 cm^2), hence scalable to wallpaper size. PlaCSH-OLED's performances can be further improved with optimized structures and materials. The work opens up many new opportunities in high-performance LEDs and displays.

Acknowledgements

S.Y.C. originated the idea of PlaCSH and PlaCSH LEDs, and initiated and directed the research. W.D. and S.Y.C. designed, fabricated and

Table 2. Contrast of PlaCSH-OLED and ITO-OLED

Structure	Luminous Reflectance (normal direction)	Contrast Ratio (CR)		
		Ambient Luminance 140 lux	Ambient Luminance 1000 lux	Ambient Luminance 10000 lux
ITO-OLED	0.67	490[a]/2300[b]	69[a]/330[b]	8[a]/34[b]
PlaCSH-OLED	0.25	2300[a]/12 000[b]	330[a]/1600[b]	33[a]/160[b]

[a]Under current density of 10 mA/cm^2; [b]Under current density of 75 mA/cm^2.

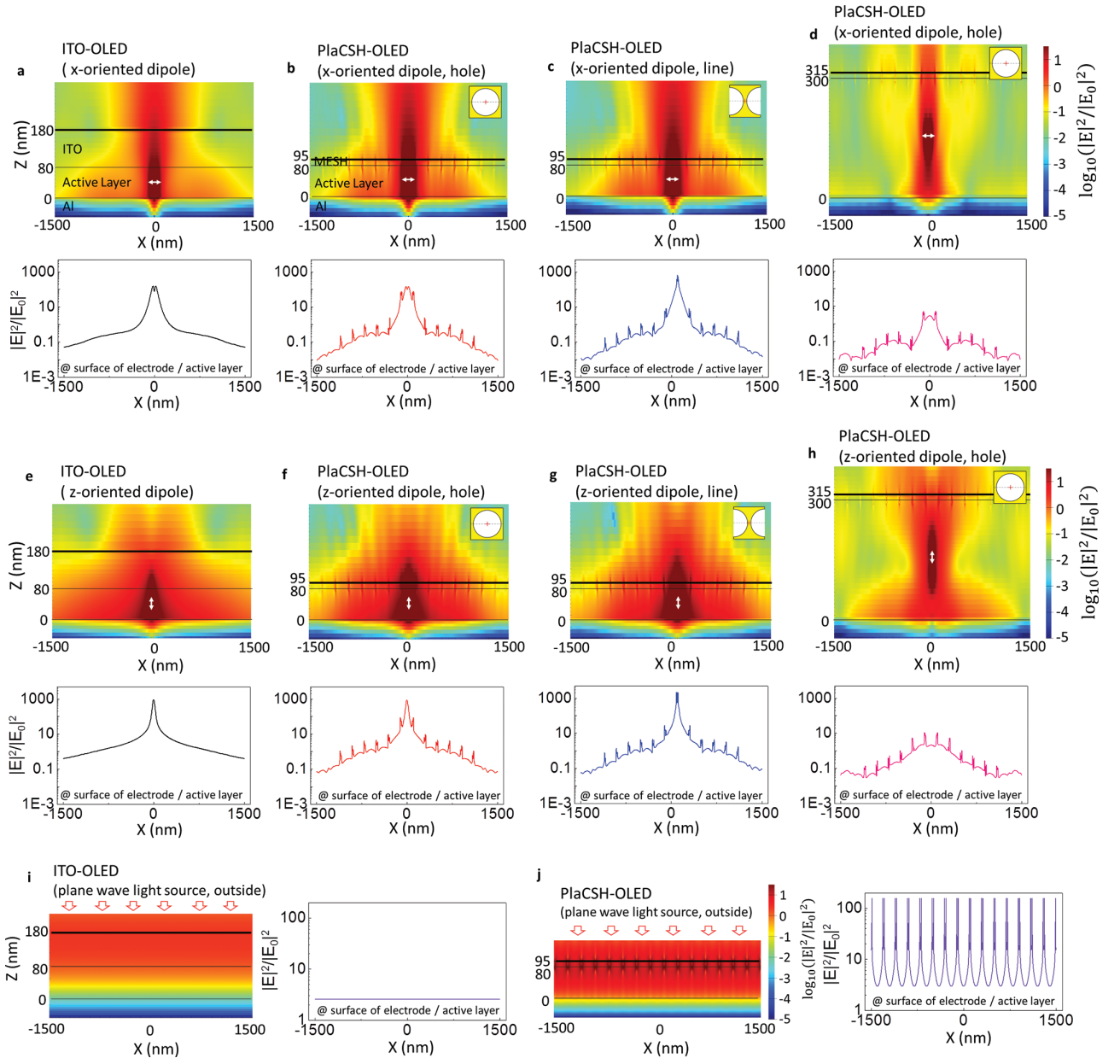

Figure 7. Numerical study of radiation and absorption properties of PlaCSH-OLED and ITO-OLED. E-field intensity distributions on a plane that is normal to the LED's layers and cuts through the center of the open-holes and grid-wire of the MESH (2D) and at the surface of the electrodes and active layer (1D) of a) ITO-OLED and PlaCSH-OLED (80 nm thick active layer) with x-oriented dipole located b) at hole and c) at grid, and d) PlaCSH-OLED with 300 nm thick active layer (dipole at hole), e–h) same as (a–d) except using *z*-oriented dipoles (all dipoles are in the middle of the light-emitting layer). i,j) E-field intensity distributions of ITO-OLED and PlaCSH-OLED (80 nm thick active layer) excited by a plane wave light source outside. In all figures, the black lines show the interface of different layers of materials. The bold line is the boundary of devices and substrate.

characterized the devices. W.D. and H. C. fabricated large area flexible mold and MESH. Y.X.W., W.D. and S.Y.C did the simulations. W.D. and S.Y.C. analyzed data. S.Y.C and W.D. wrote the manuscript. Defense Advanced Research Projects Agency (DARPA) and Office of Naval Research (ONR) for partially funding the work.

Received: March 26, 2014
Revised: May 14, 2014
Published online: August 19, 2014

[1] M. A. Baldo, D. F. O'Brien, Y. You, A. Shoustikov, S. Sibley, M. E. Thompson, S. R. Forrest, *Nature* **1998**, *395*, 151.
[2] R. H. Friend, R. W. Gymer, A. B. Holmes, J. H. Burroughes, R. N. Marks, C. Taliani, D. D. C. Bradley, D. A. Dos Santos, J. L. Bredas, M. Logdlund, W. R. Salaneck, *Nature* **1999**, *397*, 121.
[3] J. J. Wierer, A. David, M. M. Megens, *Nat. Photonics* **2009**, *3*, 163.
[4] Y. Sun, S. R. Forrest, *Nat. Photonics* **2008**, *2*, 483.
[5] W. H. Koo, S. M. Jeong, F. Araoka, K. Ishikawa, S. Nishimura, T. Toyooka, H. Takezoe, *Nat. Photonics* **2010**, *4*, 222.

[6] S. Reineke, F. Lindner, G. Schwartz, N. Seidler, K. Walzer, B. Lussem, K. Leo, *Nature* **2009**, *459*, 234.
[7] Z. B. Wang, M. G. Helander, J. Qiu, D. P. Puzzo, M. T. Greiner, Z. M. Hudson, S. Wang, Z. W. Liu, Z. H. Lu, *Nat.Photonics* **2011**, *5*, 753.
[8] R. Windisch, P. Heremans, A. Knobloch, P. Kiesel, G. H. Dohler, B. Dutta, G. Borghs, *Appl. Phys. Lett.* **1999**, *74*, 2256.
[9] M. Boroditsky, T. F. Krauss, R. Coccioli, R. Vrijen, R. Bhat, E. Yablonovitch, *Appl. Phys. Lett.* **1999**, *75*, 1036.
[10] J. J. Wierer, D. A. Steigerwald, M. R. Krames, J. J. O'Shea, M. J. Ludowise, G. Christenson, Y. C. Shen, C. Lowery, P. S. Martin, S. Subramanya, W. Gotz, N. F. Gardner, R. S. Kern, S. A. Stockman, *Appl. Phys. Lett.* **2001**, *78*, 3379.
[11] Y. R. Do, Y. C. Kim, Y. W. Song, C. O. Cho, H. Jeon, Y. J. Lee, S. H. Kim, Y. H. Lee, *Adv. Mater.* **2003**, *15*, 1214.
[12] H. M. Kim, Y. H. Cho, H. Lee, S. I. Kim, S. R. Ryu, D. Y. Kim, T. W. Kang, K. S. Chung, *Nano Lett.* **2004**, *4*, 1059.
[13] S. H. Fan, P. R. Villeneuve, J. D. Joannopoulos, E. F. Schubert, *Phys. Rev. Lett.* **1997**, *78*, 3294.
[14] I. Schnitzer, E. Yablonovitch, C. Caneau, T. J. Gmitter, A. Scherer, *Appl. Phys. Lett.* **1993**, *63*, 2174.
[15] T. Yamasaki, K. Sumioka, T. Tsutsui, *Appl. Phys. Lett.* **2000**, *76*, 1243.
[16] C. F. Madigan, M. H. Lu, J. C. Sturm, *Appl. Phys. Lett.* **2000**, *76*, 1650.
[17] Y. J. Lee, S. H. Kim, J. Huh, G. H. Kim, Y. H. Lee, S. H. Cho, Y. C. Kim, Y. R. Do, *Appl. Phys. Lett.* **2003**, *82*, 3779.
[18] T. Fujii, Y. Gao, R. Sharma, E. L. Hu, S. P. DenBaars, S. Nakamura, *Appl. Phys. Lett.* **2004**, *84*, 855.
[19] T.-W. Koh, J.-M. Choi, S. Lee, S. Yoo, *Adv. Mater.* **2010**, *22*, 1849.
[20] K. Hong, H. K. Yu, I. Lee, K. Kim, S. Kim, J.-L. Lee, *Adv. Mater.* **2010**, *22*, 4890.
[21] K. Ziemelis, *Nature* **1999**, *399*, 408.
[22] O. Renault, O. V. Salata, M. Etchells, P. J. Dobson, V. Christou, *Thin Solid Films* **2000**, *379*, 195.
[23] L. S. Hung, J. Madathil, *Adv. Mater.* **2001**, *13*, 1787.
[24] A. N. Krasnov, *Appl. Phys. Lett.* **2002**, *80*, 3853.
[25] C. D. Muller, A. Falcou, N. Reckefuss, M. Rojahn, V. Wiederhirn, P. Rudati, H. Frohne, O. Nuyken, H. Becker, K. Meerholz, *Nature* **2003**, *421*, 829.
[26] X. D. Feng, R. Khangura, Z. H. Lu, *Appl. Phys. Lett.* **2004**, *85*, 497.
[27] Z. Y. Xie, L. S. Hung, *Appl. Phys. Lett.* **2004**, *84*, 1207.
[28] S. H. Li, H. Liem, C. W. Chen, E. H. Wu, Z. Xu, Y. Yang, *Appl. Phys. Lett.* **2005**, 86.
[29] C. J. Yang, C. L. Lin, C. C. Wu, Y. H. Yeh, C. C. Cheng, Y. H. Kuo, T. H. Chen, *Appl. Phys. Lett.* **2005**, 87.
[30] K. C. Lau, W. F. Xie, H. Y. Sun, C. S. Lee, S. T. Lee, *Appl. Phys. Lett.* **2006**, 88.
[31] Y. C. Zhou, L. L. Ma, J. Zhou, X. D. Gao, H. R. Wu, X. M. Ding, X. Y. Hou, *Appl. Phys. Lett.* **2006**, 88.
[32] S. F. Chen, J. Xie, Y. Yang, C. Y. Chen, W. Huang, *J. Phys. D. Appl. Phys.* **2010**, 43.
[33] G. H. Xie, Z. S. Zhang, Q. Xue, S. M. Zhang, L. Zhao, Y. Luo, P. Chen, B. F. Quan, Y. Zhao, S. Y. Liu, *Org. Electron.* **2010**, *11*, 2055.
[34] S. Y. Kim, J. H. Lee, J. H. Lee, J. J. Kim, *Org. Electron.* **2012**, *13*, 826.
[35] J. J. Liang, L. Li, X. F. Niu, Z. B. Yu, Q. B. Pei, *Nat. Photonics* **2013**, *7*, 817.
[36] V. Bulovic, V. B. Khalfin, G. Gu, P. E. Burrows, D. Z. Garbuzov, S. R. Forrest, *Phys. Rev. B* **1998**, *58*, 3730.
[37] A. Dodabalapur, L. J. Rothberg, R. H. Jordan, T. M. Miller, R. E. Slusher, J. M. Phillips, *J. Appl. Phys.* **1996**, *80*, 69, 54.
[38] Y. J. Lee, J. M. Hwang, T. C. Hsu, M. H. Hsieh, M. J. Jou, B. J. Lee, T. C. Lu, H. C. Kuo, S. C. Wang, *Ieee Photonics Tech. Lett.* **2006**, *18*, 1152.
[39] T. Tsutsui, M. Yahiro, H. Yokogawa, K. Kawano, *Adv. Mater.* **2001**, *13*, 1149.
[40] E. F. Schubert, N. E. J. Hunt, M. Micovic, R. J. Malik, D. L. Sivco, A. Y. Cho, G. J. Zydzik, *Science* **1994**, *265*, 943.
[41] N. C. Greenham, R. H. Friend, D. D. C. Bradley, *Adv. Mater.* **1994**, *6*, 491.
[42] Y. Gu, L. J. Wang, P. Ren, J. X. Zhang, T. C. Zhang, O. J. F. Martin, Q. H. Gong, *Nano Lett.* **2012**, *12*, 2488.
[43] W. L. Barnes, *J. Lightwave Technol.* **1999**, *17*, 2170.
[44] K. Y. Yang, K. C. Choi, C. W. Ahn, *Appl. Phys. Lett.* **2009**, 94.
[45] J. Vuckovic, M. Loncar, A. Scherer, *IEEE J. Quantum Elect.* **2000**, *36*, 1131.
[46] C. Liu, V. Kamaev, Z. V. Vardeny, *Appl. Phys. Lett.* **2005**, 86.
[47] S. Y. Chou, W. Ding, *Opt. Express* **2013**, *21*, A60.
[48] W. D. Li, J. Hu, S. Y. Chou, *Opt. Express* **2011**, *19*, 21098.
[49] S. Y. Chou, P. R. Krauss, P. J. Renstrom, *Science* **1996**, *272*, 85.
[50] H. Tan, A. Gilbertson, S. Y. Chou, *J. Vac. Sci. Technol. B* **1998**, *16*, 3926.
[51] S. Y. Chou, Q. F. Xia, *Nat. Nanotechnol.* **2008**, *3*, 295.
[52] M. G. Helander, Z. B. Wang, M. T. Greiner, Z. W. Liu, J. Qiu, Z. H. Lu, *Adv. Mater.* **2010**, *22*, 2037.
[53] G. Gu, D. Z. Garbuzov, P. E. Burrows, S. Venkatesh, S. R. Forrest, M. E. Thompson, *Opt. Lett.* **1997**, *22*, 396.
[54] N. C. Erickson, R. J. Holmes, *Appl. Phys. Lett.* **2010**, *97*, 083308.
[55] E. Ozbay, *Science* **2006**, *311*, 189.
[56] J. A. Schuller, E. S. Barnard, W. Cai, Y. C. Jun, J. S. White, M. L. Brongersma, *Nat. Mater.* **2010**, *9*, 193.